INSTITUTE OF PHYSICS PUBLISHING SMART MATERIALS AND STRUCTURES
Smart Mater. Struct. **15** (2006) S14–S20 doi:10.1088/0964-1726/15/1/004

Passive wireless sensors using electrical transition of carbon nanotube junctions in polymer matrix

Hargsoon Yoon[1,3], **Jining Xie**[1], **Jose K Abraham**[1], **Vijay K Varadan**[1] **and Paul B Ruffin**[2]

[1] Center for the Engineering of Electronic and Acoustic Materials and Devices, Pennsylvania State University, University Park, PA 16802, USA
[2] US Army Aviation and Missile Research, Development, and Engineering Center, Redstone Arsenal, AL 35898, USA

Received 7 December 2004, in final form 17 June 2005
Published 13 December 2005
Online at stacks.iop.org/SMS/15/S14

Abstract
This paper presents the design and development of a passive wireless sensor for the detection of bio-hazard materials and vapors using chemiresistive thin films. Composite polymer thin film with functionalized carbon nanotubes (f-CNT) and polymethylmethacrylate (PMMA) is employed as a sensing material. It is investigated that resistance change is determined with the concentration of dichloromethane vapors diffused into composite thin film, due to electrical transition from direct contact to tunneling in carbon nanotube nanojunctions. The chemiresistive film is integrated into a passive wireless system which works based on the change in phase of the reflected RF signal. Measurement results of sensors in a wireless sensing system show a large differential phase shift, which can be utilized for remote monitoring of bio-hazard vapors in real time.

(Some figures in this article are in colour only in the electronic version)

1. Introduction

The present nanosensor research offers unprecedented opportunities to utilize relevant mechanical, chemical, thermal, chromatographic, magnetic, biological, and/or acoustic phenomena for sensors and sensor network development. Sensors based on nanoscale properties have various advantages over macroscale sensors including small size, high sensitivity and high selectivity that are essential factors for realization of new sensors for applications such as human health care, national security and environmental safety. In addition, advanced technologies for sensor fabrication and integration with other electronic components will enable miniaturization, reduction of cost and less power consumption. Even though the influence of nanotechnology on sensor research is enormous, efforts to date have focused primarily on the physical and chemical properties of host materials in nanoscale. For example, individual silicon/tin oxide nanowires were utilized for nanoscale biological/chemical sensors using their own characteristics in nanoscale dimension. Although this is an attractive feature due to high sensitivity at a molecular level, the technology of these nanowire sensors for mass production is limited, because of difficulty in integration into electronic circuits. Thus, several approaches are being investigated to develop solutions for integration of nanotechnology into electronic devices for sensing applications [1–3].

Development of a new method for highly selective and sensitive detection of organic vapors based on carbon nanotubes and gold nanowires is presented in [4] utilizing the properties of an atomic-scale electrical junction between nanotubes/wires in a polymer matrix. As shown in figure 1, when the polymer matrix is exposed to sensing molecules, the reaction between the molecules and the matrix material changes the physical properties and dimensions of the polymer matrix. Physical distance change between nanowires due to swelling is considered as one of the most common responses. Even though the distance change is only a few ångströms, it will lead to a significant transition of electrical junctions from direct

[3] Present address: High Density Electronic Center and Department of Electrical Engineering, University of Arkansas, Fayetteville, AR 72701, USA.

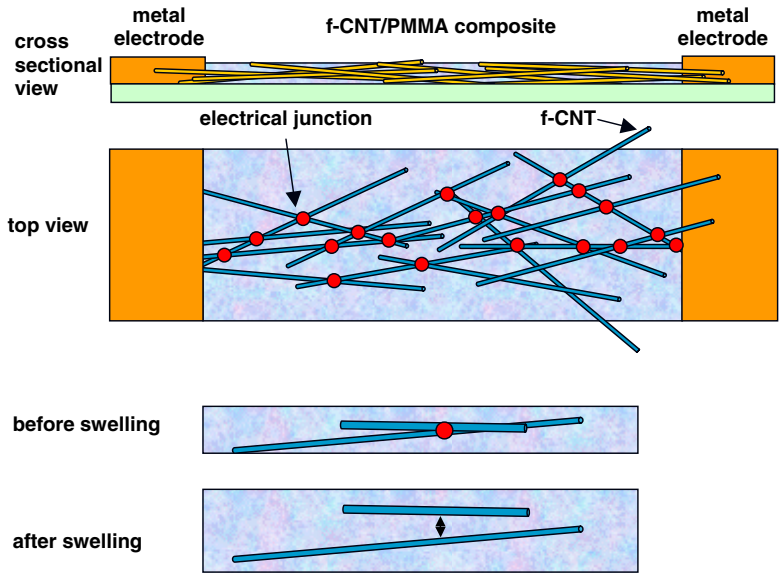

Figure 1. Schematic diagram of junction resistance change between two nanowires due to polymer matrix swelling.

contact to the tunneling regime in between carbon nanotubes and the electrical property change of the whole sensor film will be quite high. The number of source molecules and the interaction parameter with the matrix material determines the extent of matrix swelling and resistance variation [5]. It could be possible to choose proper materials for matrix selective sensors for the detection of various gases. Based on this concept, several composite films with gold nanowires and carbon nanotubes were developed. One of the interesting materials is the functionalized carbon nanotube (f-CNT) composite with polymethyl methacrylate (PMMA). Electrons flow through conducting carbon nanotubes that are randomly distributed and contacted onto electrodes. The number and length of conducting paths and electrical properties of junctions formed inside f-CNT/polymer composites will determine the conductance of composite thin films.

Along with the development of nanoscale sensors, their integration with electronic circuits for detection and identification, especially using wireless communication devices, can find significant impact in a broad range of applications. The integration of nanoscale sensors into wireless communication networks will provide wide opportunities for biological sensor applications, especially for real-time physiological sensing of human health and bio-hazard material detection using personal mobile stations and internet services. The convergence of the advanced technologies in nanoscale sensors and wireless communications will open up vast opportunities for a variety of sensor systems.

The urgent need for sensors for various applications has triggered the integration of sensors with active wireless devices with data processing, communication components and a battery as the power source in addition to the inherent sensing components [6]. Even these attempts have been successful and met special requirements in field applications; issues for long term monitoring outside battery lifetime still remain. Ong *et al* demonstrated that CNT-based sensors on inductor–capacitor (LC) resonators are capable of remote detection of inorganic gases such as CO_2 and O_2 [7]. Chopra *et al* reported a selective gas detection system based on Cu disk resonators with carbon nanotubes using LC resonant circuits [8]. However, those methods using LC resonators require close proximity of large loop antennas, which has space as well as distance constraints. In this paper we report the design, development and experimental results of nanowire and nanotube composite sensors integrated with a passive wireless system for remote and real time monitoring. The passive wireless system is based on the principle of reflecting electromagnetic waves from the sensor and sending them back to the transceiver antenna.

2. Polymer/nanotube composite sensor fabrication and measurements

2.1. f-CNT/PMMA composite sensor design and fabrication

The sensor film is fabricated using functionalized CNT/PMMA composites. CNTs were synthesized by the decomposition of acetylene gas by microwave chemical vapor deposition at 600 °C with fine iron nanoparticles as a catalyst. Carbon nanotubes were functionalized with potassium permanganate and acetic acid. Composite thin films were prepared by ultrasonication of 10 mg f-CNTs and 90 mg PMMA in 2 ml dichloromethane for 2 h [9].

The typical evaluation of a sensor is to measure its output responses either in voltage (amplitude, phase) or change in frequency. It is well known that for any RF measurement devices the change in phase can give a better accuracy and sensitivity. The phase change is obtained in the present method by utilizing the reflected RF signals from bilateral interdigital coplanar waveguides. Composite thin films were fabricated on a high frequency transmission line with coplanar waveguides, because of its simple structure and ease of application of resistive thin film for a terminated load. Also, bilateral interdigital fingers were used in this design to get more sensing area as well as to increase the number of conducting contacts

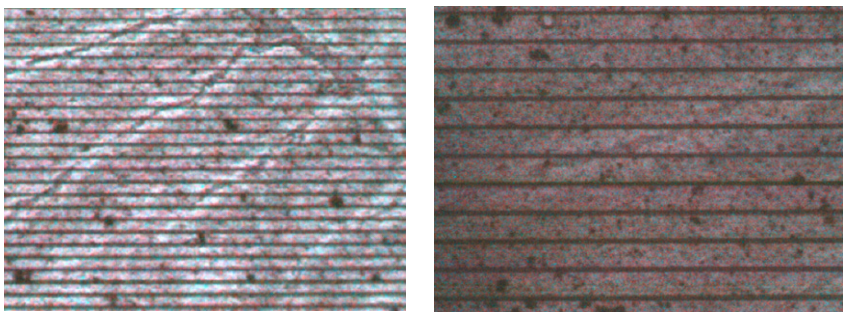

Figure 2. Photographs of f-CNT/PMMA composite on an interdigital electrode.

between carbon nanotubes and metal electrodes. Coplanar waveguides with interdigital fingers were fabricated using photo-lithography and a wet etching process. After fabrication of the coplanar waveguide, the composite solution was spin-coated at 2000 rpm onto a coplanar waveguide with interdigital fingers to develop it as a resistive load. The sensors were dried at 50 °C in air. Figure 2 presents the photograph of a fabricated sensor with f-CNT/PMMA thin film.

2.2. *Sensor characterization*

The responses of f-CNT/PMMA composite sensors for different gas concentrations were measured using conventional resistance measurement methods by placing the sensor inside a gas chamber and exposing to different gases. The sensors were exposed to air after its saturation level. Changes in resistance due to change in gas concentrations and exposure time were also measured.

As shown in figure 3, the resistance of CNT/PMMA composite thin film rapidly increased with dichloromethane vapor concentration. It is observed that the resistance of the composite in figure 3(a) increased with gas concentration and reached saturated values within 10 min. The resistance increase is regarded as being caused by the free volume change of the PMMA polymer matrix. The volume change is determined by the exposure time and concentration of dichloromethane vapor. Because lateral expansion of polymer is negligible compared to the vertical direction, the volume change of swollen polymer can be described as the increase in thickness of the polymer matrix. Due to the matrix swelling, the gap between the electrical junctions between the conducting carbon nanotubes increases and becomes wider. According to Flory–Huggins theory and a modified Raoult's law [5], the thickness increase Δt corresponding to small solvent content can be given as

$$\Delta t = (t_{\mathrm{solv}} - t_{\mathrm{dry}}) \cong \mathrm{e}^{-(1+\chi)} t_{\mathrm{dry}} \frac{P_{\mathrm{s}}}{P_{\mathrm{s}}^{\mathrm{sat}}} \qquad (1)$$

where t_{solv} is the thickness in solvent vapor, t_{dry} is the original thickness, χ is the Flory–Huggins polymer–solvent interaction parameter, P_{s} is the partial pressure of the solvent vapor, and $P_{\mathrm{s}}^{\mathrm{sat}}$ is the saturated vapor pressure of the solvent vapor. This relationship indicates that the thickness increase by solvent vapor diffusion in polymer matrix is linear with solvent vapor pressure. If we assume uniform swelling of polymer composite after saturation, the distance change between two carbon nanotubes Δs is expected as a linear function of solvent vapor pressure, as well.

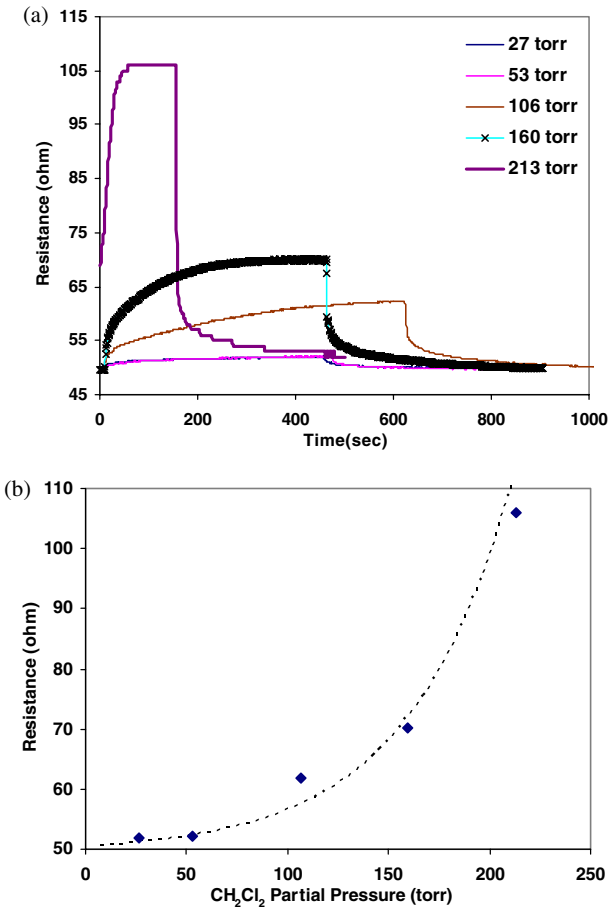

Figure 3. (a) Measured resistance change due to change in expose time for different concentrations and (b) saturated resistance with partial pressure of dichloromethane vapor.

As illustrated in figure 3(b), the experimental data for static resistance after saturation was found to be best fitted by a relation of the form

$$\Delta R = \exp(\alpha P_{\mathrm{s}}) \qquad (2)$$

for the resistance increase ΔR as a function of partial pressure P_{s}, where ΔR is in ohms and P_{s} in Torr. The fitting parameter α for the f-CNF/PMMA composite is 0.0195. Based on the measurement results, it is expected that there is an

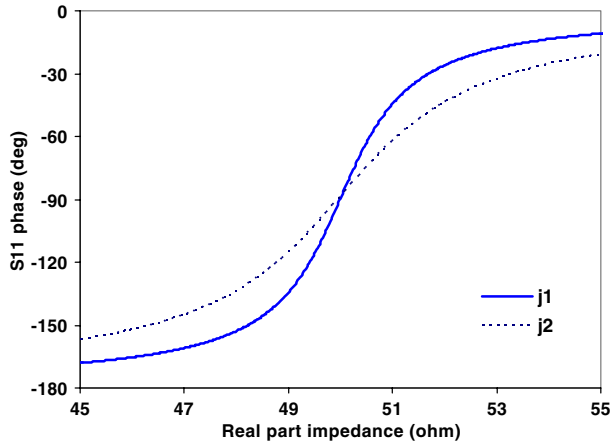

Figure 4. Reflection (S11) phase related to real and imaginary parts of load impedance ($Z_L = a + jb$): $z_1 = a + j1$ and $z_2 = a + j2$.

exponential dependence between the resistance change ΔR and the distance change between two carbon nanotubes Δs. According to the Simmons formalism based on the same metal electrodes [10], tunneling electron current density J_{tunnel} is given by

$$J_{\text{tunnel}} = \left(\frac{e}{2\pi h \Delta s^2}\right)\left\{\left(\Phi_0 - \frac{eV}{2}\right) \times \exp\left[-\frac{4\pi\Delta s}{h}\left(2m_e\left(\Phi_0 - \frac{eV}{2}\right)\right)^{1/2}\right] - \left(\Phi_0 + \frac{eV}{2}\right)\exp\left[-\frac{4\pi\Delta s}{h}\left(2m_e\left(\Phi_0 + \frac{eV}{2}\right)\right)^{1/2}\right]\right\} \tag{3}$$

where e is the charge of an electron, h is Planck's constant, Φ_0 is the height of the potential barrier, and V is the voltage across the insulating layer. It is important to realize from equation (3) that there is an exponential dependence between the tunneling current and the distance between two electrodes, agreeing well with our measurement results. Even atomic-scale changes in distance will lead to a significant change in current flow and this explains the sensor response to the concentration of solvent vapors.

3. Wireless sensing and measurements

3.1. Computation of change in phase of the reflected wave

Based on the sensor response of resistance change in f-CNT/PMMA composite, we proposed a wireless sensing method [11]. When a reflected wave exists on a lossless transmission line terminated with a load impedance $Z_L = a + jb$, the voltage across the line can be given by [12]

$$V = V^+ e^{-j\beta z} + V^- e^{j\beta z} \tag{4}$$

where V^+ and V^- are amplitude constants of incident and reflected waves, and β is a phase constant for the lossless line. The voltage reflection coefficient Γ_L is described by the ratio of V_- to V_+:

$$\Gamma_L = \frac{V^-}{V^+} = \frac{Z_L - Z_C}{Z_L + Z_C} \tag{5}$$

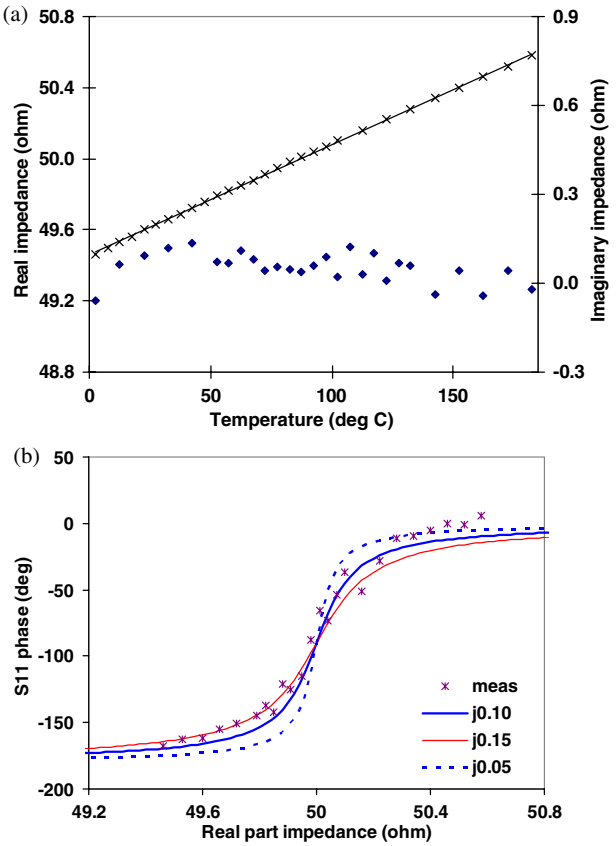

Figure 5. (a) Real and imaginary parts of impedance with temperature and (b) comparison of measured and calculated phase shifts with impedances of the thermistor.

and voltage at any point on the transmission line ($z < 0$) is given by

$$V = V^+(e^{-j\beta z} + |\Gamma_L|e^{j(\theta+\beta z)}) \tag{6}$$

$$\Gamma_L = |\Gamma_L|e^{j\theta} \tag{7}$$

$$|\Gamma_L| = \frac{[(a^2 + b^2 - Z_c^2)^2 + 4b^2 Z_c^2]^{1/2}}{(a + Z_c)^2 + b^2} \tag{8}$$

$$\theta = \sin^{-1}\left\{\frac{a^2 + b^2 - Z_c^2}{\sqrt{(a^2 + b^2 - Z_c^2)^2 + 4b^2 Z_c^2}}\right\} \tag{9}$$

where Z_c is the characteristic impedance of the transmission line.

It can be seen from equation (9) that the phase of the reflected wave in a transmission line can be determined by the load impedance. The change in phase of a reflected wave with respect to load impedances of a transmission line is illustrated in figure 4. As long as the imaginary part of the load impedance is low, the reflected wave phase exhibits large phase shift with small change in the real part of the load impedance near the characteristic impedance.

In order to check the validity of the analytical formula, we tested a thermistor with a network analyzer (HP8510C) and compared with calculation. Based on the characteristics of the thermistor, linear variation in resistance from 0 to 180 °C temperature change can be obtained. As shown in figure 5(a), real parts from 49.46 to 50.58 and imaginary

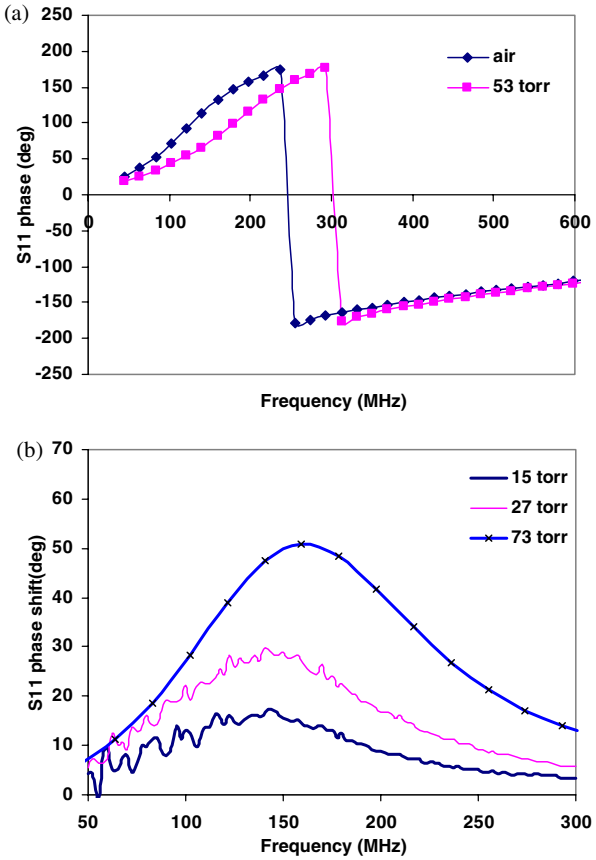

Figure 6. (a) Measured reflection phase (S11) in air and 53 Torr dichloromethane vapor and (b) differential phase shift when the sensor is exposed to dichloromethane vapor with different partial pressures (15, 27 and 53 Torr).

parts of impedances from −0.05 to 0.15 were measured by an impedance analyzer (HP4192A). For each impedance value, we measured the phase shifts of the reflected wave at 400 MHz frequency using the network analyzer. Due to the change in resistance, the phase change of the reflected wave was observed and agreed well with the calculations as shown in figure 5(b).

3.2. Reflection phase measurements

Based upon the principle and measured results, the reflected phase was measured to detect a small variation of dichloromethane concentration. In this measurement, dichloromethane vapors with three different concentrations (15, 27, and 53 Torr partial pressures) were introduced into a vapor test chamber and the reflected wave phase was monitored by the network analyzer. Figure 6(a) shows the S11 phase response of a sensor with CNT/PMMA composite from 50 to 600 MHz. It was clearly shown that the phase of the reflected wave in 53 Torr dichloromethane vapor was shifted from the original value in air, due to resistance increase in the composite thin film. Since the reflected phases rapidly change around 150 MHz and the resolution of sensing is high enough, concentration changes from 15 to 53 Torr of dichloromethane vapor partial pressure were clearly detected. In DC resistance measurement, the difference was hardly detected, even hindered by noise. It is shown

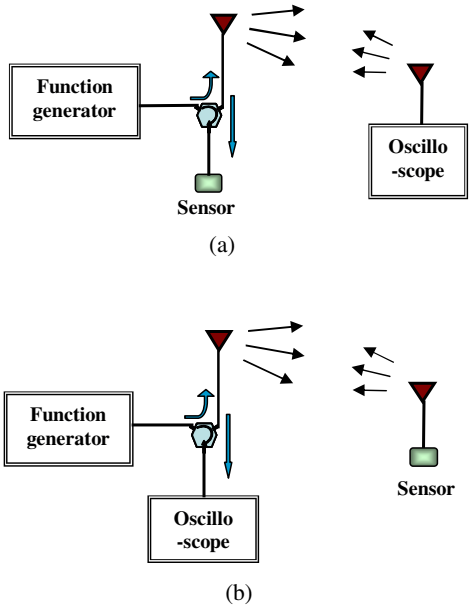

Figure 7. Schematic diagram of a wireless sensing system: (a) with signal source and (b) without signal source.

Table 1. Measured and calculated phase change from reference loads.

	Measured input impedance		Received differential phase	
Resistance	Real	Imaginary	Measured	Calculated
L1 Short	2.4	−2.0	−166.3	−175.4
L2 17 Ω	20.5	13.9	−139	−143.6
L3 25 Ω	27.1	9.6	−117.4	−151.2
L4 50 Ω	50.3	1.7	−40.3	−80.1
L5 100 Ω	90.1	−14.0	3.6	−13.5
L6 Open	285.3	502.4	0	−8.6

that the electromagnetic wave property from reflected phase measurement is useful for chemiresistor sensors with high sensitivity, in addition to the possibility of wireless sensing implementation.

3.3. Wireless gas sensing measurements

After the measurement of sensors directly connected to a vector network analyzer, sensors were characterized in a wireless test system, as shown in figure 7. The wireless test system consists of a function generator (HP8647A), an oscilloscope (TDS2022), an RF circulator and two antennas. The function generator delivers a sinusoidal RF signal to the sensor through a circulator and an RF signal reflected back from the sensor is sent to the antenna through the circulator. The electromagnetic waves from the sensor are received by the antenna, which is connected to an oscilloscope. Phase and amplitude differences with vapor exposure time and various concentrations are measured using the oscilloscope and recorded using software (Wavestar v.2.8.1) and a TDSCMAX communication module.

Before measurement of phase variation inside the gas chamber, preliminary tests using reference loads in table 1

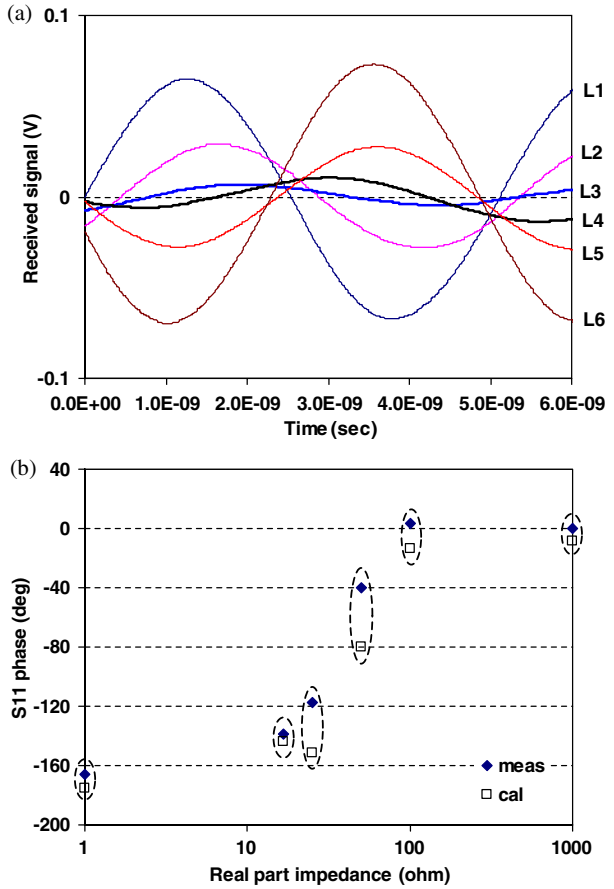

Figure 8. (a) Received signals versus time and (b) differential phase shifts for reference loads with respect to L6.

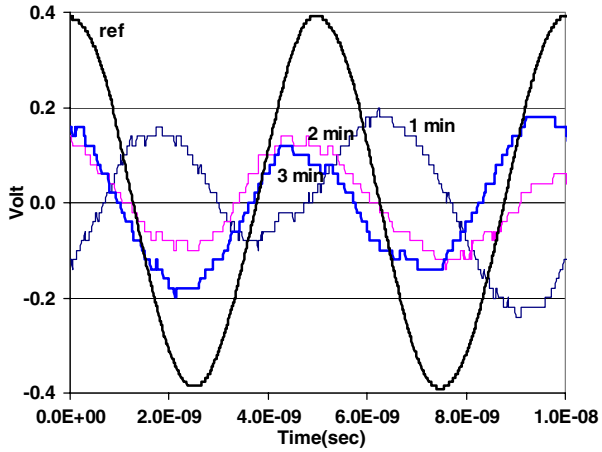

Figure 9. Measured reflected signal from the sensor with respect to exposed time (1, 2, and 3 min).

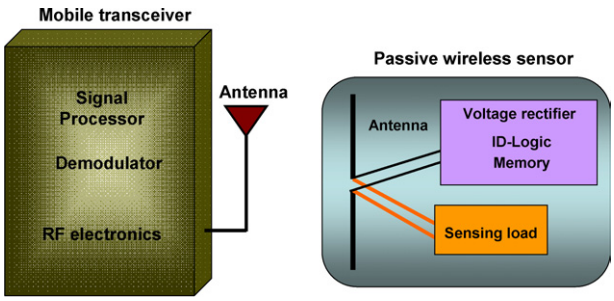

Figure 10. Schematic diagram of passive wireless sensor integrated with RFID.

were performed in the wireless network. The purpose of preliminary tests was to check whether the wireless test system works properly. 200 MHz sinusoidal signal was chosen as an input signal. To check reflection phases depending on the load impedance, reference loads (L1, L2, L3, L4, L5, and L6) with various impedance values were connected to the termination port of the circulator and measured as shown in figure 8(a). The signals from reference loads demonstrated phase shift and signal intensity change depending on the impedance of each load. When terminal impedance changed from short (L1) to open (L6), differential phase increased from −166° to 0°. This agreed well with the analytical calculation using equation (9), as shown in figure 8(b).

F-CNT/PMMA composite sensors in dichloromethane vapors were measured using the same system. Figure 9 demonstrates that the differential phase increases with respect to the gas expose time. The sensor measured in this experiment has 26 Ω initial resistance before it is exposed to the vapors. As seen from the data presented in figure 9, rapid impedance change was observed up to 2 min exposure. It is considered that the large phase shift was caused by rapid impedance changes near the characteristic impedance. The rapid impedance change at the initial period of exposure was shown in previous measurements also. The slow increase of phase shift after 2 min exposure is regarded as the impedance being close to saturation. The same kind of behavior was also observed in DC resistance measurement at high concentration of dichloromethane vapors. With this experiment, the concept of this wireless network and possible applications were clearly demonstrated.

A compact design of passive wireless sensors without any RF circulator for industrial and mobile sensing application is presented in figure 10 using an RFID (radio frequency identifications system). Since the data are inherently embedded in noise, further investigation of signal detection is required, which is progressing.

4. Conclusions

In this paper, we have presented the development of chemiresistive sensors for detection of bio-hazardous materials. This passive wireless sensor is based on monitoring the phase of the reflected RF signal from a functionalized CNT/PMMA composite thin film, which is coated on an interdigital coplanar waveguide. It was observed that the resistance change is due to the change in concentration of dichloromethane vapor and hence the conducting mechanism of the chemiresistor is governed by the tunneling effect. Different gas concentrations affect the distance between conducting carbon nanotubes by diffusion of molecules into the composite thin film. With the measurements on the reflected phase from the sensor, we clearly demonstrated the possibility of using it as a passive sensor without any battery at the sensor. Measured results of sensors and reference loads in the wireless

sensing system show large differential phase shifts, which can be utilized for real-time remote monitoring of bio-hazardous vapors.

References

[1] Cui Y, Wei Q, Park H and Lieber C M 2001 Nanowire nanosensors for highly sensitive and selective detection of biological and chemical species *Science* **293** 1289–92

[2] Lin Y, Lu F, Tu Y and Ren Z 2003 Glucose biosensors based on carbon nanotube nanoelectrode ensembles *Nano Lett.* **4** 191–5

[3] Nguyen P, Ng H T, Yamada T, Smith M K, Li J, Han J and Meyyappan M 2004 Direct integration of metal oxide nanowire in vertical field effect transistor *Nano Lett.* **4** 651–7

[4] Yoon H, Philip B, Abraham J K, Ji T and Varadan V K 2005 Nanowire sensor array for wireless detection and identification of bio-hazards *Proc. SPIE Conf. on Smart Elec. MEMS, BioMEMS, and Nanotech.* **5763** 326–32

[5] Graves-Abe T, Pschenitzka F, Jin H Z, Bollman B, Sturm J C and Register R A 2004 Solvent-enhanced dye diffusion in polymer thin films for polymer light-emitting diode application *J. Appl. Phys.* **96** 7154–63

[6] Abraham J K, Philip B, Whitchurch A, Varadan V K and Reddy C C 2004 A compact wireless gas sensor using a carbon nanotube/PMMA thin film chemiresistor *Smart Mater. Struct.* **13** 1045–9

[7] Ong K G, Zeng K and Grimes C A 2002 A wireless, passive carbon nanotube-based gas sensor *IEEE Sensors J.* **2** 82–8

[8] Chopra S, McGuire K, Gothard N, Rao A M and Pham A 2004 Selective gas detection using a carbon nanotube sensor *Appl. Phys. Lett.* **83** 2280–2

[9] Zhang N, Xie J and Varadan V K 2002 Functionalization of carbon nanotubes by potassium permanganate assisted with phase transfer catalyst *Smart Mater. Struct.* **11** 962–5

[10] Simmons J G 1963 Generalized formula for the electric tunnel effect between similar electrodes separated by a thin insulating film. *J. Appl. Phys.* **34** 1793

[11] Yoon H, Philip B, Xie J, Ji T and Varadan V K 2004 Nanowire sensor applications based on radio frequency phase shift in coplanar waveguide *Proc. SPIE Smart Struct. Mater.* **5389** 101–7

[12] Collin R E 1992 *Foundations for Microwave Engineering* (New York: McGraw-Hill)